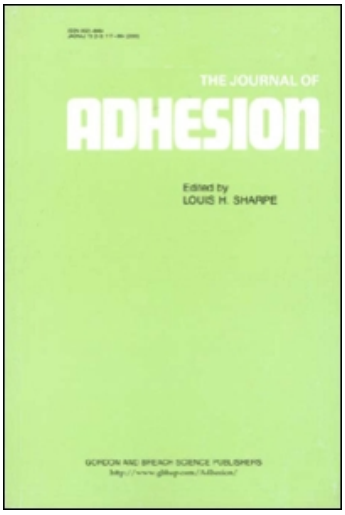

The Journal of Adhesion
Publication details, including instructions for authors and subscription information:
http://www.informaworld.com/smpp/title~content=t713453635

Adhesion of Nanoparticles Fouling Glass Surfaces

K. Kendall[a]; M. R. Kosseva[a]
[a] Chemical Engineering, University of Birmingham, UK

To cite this Article Kendall, K. and Kosseva, M. R.(2005) 'Adhesion of Nanoparticles Fouling Glass Surfaces', The Journal of Adhesion, 81: 10, 1017 — 1030
To link to this Article: DOI: 10.1080/00218460500310739
URL: http://dx.doi.org/10.1080/00218460500310739

The Journal of Adhesion, 81:1017–1030, 2005

ISSN: 0021-8464 print/1545-5823 online
DOI: 10.1080/00218460500310739

Taylor & Francis
Taylor & Francis Group

Adhesion of Nanoparticles Fouling Glass Surfaces

K. Kendall
M. R. Kosseva
Chemical Engineering, University of Birmingham, UK

The fouling of glass surfaces by nanoparticles formed from corroding iron was studied. Simple experiments demonstrated that adherent films of nanoparticles were deposited by corrosion of iron particles on a glass surface and by flowing water past corroding particles and then onto a glass surface. The water collected from this experiment was found to contain about 2 parts per million (ppm) of particles 500 nm in diameter when tested by photon correlation spectroscopy. However, electron micrographs showed that the primary particles in the fouling film were 20 nm in diameter. This discrepancy was explained by a new theory of nucleation of the fouling films. The theory was confirmed by measuring the particle size of ferric hydroxide dispersions as a function of concentration and pH. It was shown that the 20 nm primary nanoparticles nucleated much larger stable aggregates (defined as nucleags), which were sensitive both to pH and to magnetic fields. In particular, as the pH rose above 6, flocculation occurred, and large unstable agglomerates were observed. The conclusion was that three types of particle could exist in the corrosion product of iron and water: nanoparticles, nucleags, and flocs.

Keywords: Adhesion of particles; Colloid stability; Flocculation; Fouling of glass; Fouling of surfaces; Nanoparticle aggregates; Nanoparticles; Nucleags

1. INTRODUCTION

The objective of this article is to describe experiments on the adhesion of nanoparticles that conform to the criteria found in the work of Ghatak *et al*. that the demonstrations should be simple, easily

Received 10 February 2005; in final form 9 May 2005.
One of a collection of papers honoring Manoj K. Chaudhury, the February 2005 recipient of The Adhesion Society Award for Excellence in Adhesion Science, sponsored by 3M.
Presented in part at the 28th Annual Meeting of the Adhesion Society, Mobile, Alabama, USA, 13–16 February 2005.
Address correspondence to Kevin Kendall, University of Birmingham, School of Chemical Engineering, Edgbaston, B15 2TT, UK. E-mail: k.kendall@bham.ac.uk

constructed, readily visible, and capable of new theoretical interpretation [1]. In the field of nanoparticle adhesion, this is difficult because the particles are so small, typically 10,000 times smaller than individual particles visible to the naked eye.

However, nanoparticles are visible when they are adhered together and used as surface layers in the polymer-film and metal-coating industries [2–6]. Examples are silica nanoparticles used in the surface treatment of poly ethylene terephthalate films and polymer latex paints used in metal-surface protection. Concrete, the world's biggest bulk commodity, hardens and gains its strength from the adhesion of calcium silicate hydrate nanoparticles, which glue the larger sand grains and rocks together [7]. The nanoparticle films formed from cement can be readily seen in reflected light on a water surface as a white film next to a hydrating cement body.

In the same way, the nanoparticles responsible for fouling glass surfaces are easily seen by the naked eye because they deposit ugly brown stains on windows and walls of buildings. In reflection, these films can exhibit interference colours of white, blue, and red, indicating that the film thickness is around 100 nm. Where steel, copper, or lead sheets have been used in roofing applications, brown, green, or grey streaks are visible on the walls where water has run off the metal. If water systems are built of metal, with copper or steel pipes, colored corrosion films can be seen on ceramic basins and lavatories. These are strongly adherent and require acid treatment (e.g., oxalic acid) for removal [8, 9].

The purpose of this article is to investigate the nucleation and growth of these nanoparticle corrosion fouling films. First, preliminary observations show that the films are of three types: 20 nm structured, 200 nm structured, and flocculated. A new theory is proposed to account for the nucleation of the films. Then, experiments on controlled ferric hydroxide nanoparticle dispersions show that the deposition is highly sensitive to pH and magnetic fields.

2. PRELIMINARY OBSERVATIONS

Two experiments were set up to display the fouling process (Figure 1). The first consisted of a drop of water on a glass microscope slide onto which iron filings had been sprinkled (Figure 1a). The second was a glass slide onto which water was dripped through a rubber tube filled with steel wool (Figure 1b).

After several hours, corrosion products could be seen on the glass slides. These were observed by reflection optical microscopy, which revealed thin films of ferric hydroxide [10] deposited on the surfaces. When wet, these were readily scratched, but after drying they

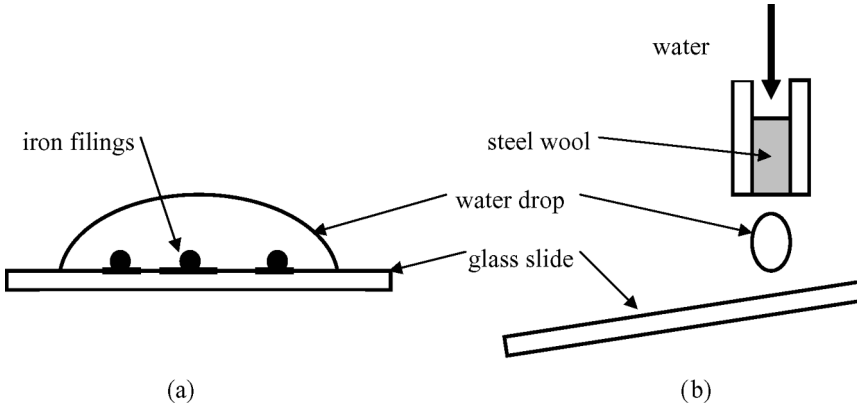

FIGURE 1 a) Water drop on glass slide with iron particles; b) water drop impinging on a glass slide after passing through steel wool.

adhered tenaciously to the glass surface. The micrograph shown in Figure 2 revealed that there were two types of material on the glass. The first was a fine structured film, which could be extremely thin and appeared white in the micrograph. The second was a thicker coloured film around 200 nm in thickness. Third, there was an amorphous brown deposit, which had flocculated in the suspension

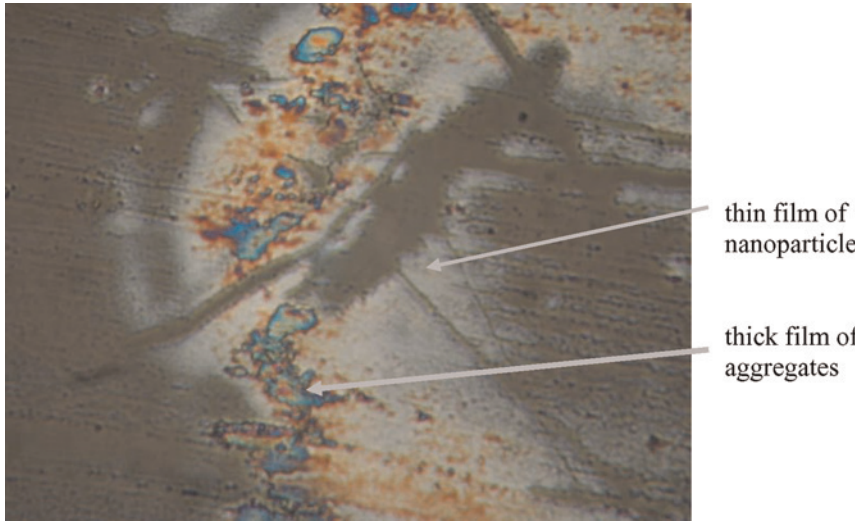

FIGURE 2 Reflection micrograph of fouling film on glass slide.

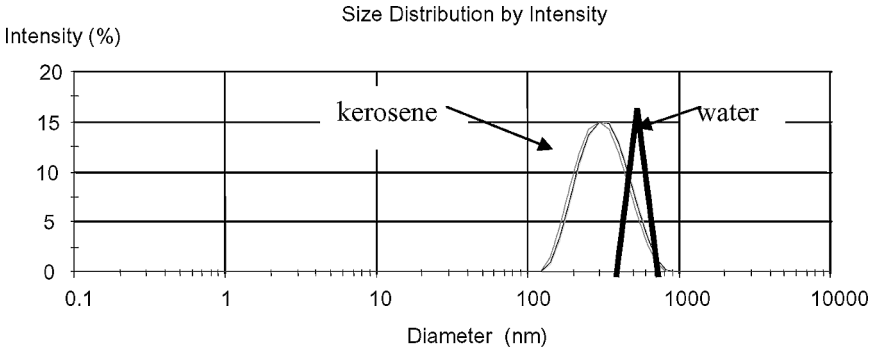

FIGURE 3 PCS results for water causing the fouling deposit.

and subsequently dropped onto the glass surface, which had been cleaned from the surface shown in Figure 2 by wiping with a wet tissue. The first two films were strongly adherent and could not be removed with the tissue.

The water at pH 7.1 running over the glass was collected and analysed for iron. It contained 2 ppm. Fine brown flocs could be seen in it, and these sedimented to the bottom of the container. The same size of particle was found in other liquids such as kerosene, which had been stored in steel drums. Photon correlation spectroscopy (PCS) [11] showed that the colloid particles were between 200 and 800 nm in diameter as shown in Figure 3, rather similar to those found in kerosene. This was surprising because transmission electron microscopy showed the fouling film to be composed of 20 nm particles. How did these larger entities, apparently aggregates, form from the 20 nm nanoparticles?

A new theory was first proposed to explain the formation of these aggregates and deposition of the nanoparticle films. Then, experiments were carried out on well-characterised ferric hydroxide nanoparticles to verify the theory, varying pH and magnetic field. Finally, conclusions about nanoparticle adhesion of fouling films were drawn.

3. THEORY

The mechanism explaining the deposition of nanoparticle fouling films on glass surfaces is shown in Figure 4. An iron particle sitting on a glass surface is covered by a water droplet and oxygen diffuses to it from the surrounding air, allowing corrosion of the iron to start [9]. Under appropriate pH conditions, electrochemical reaction between

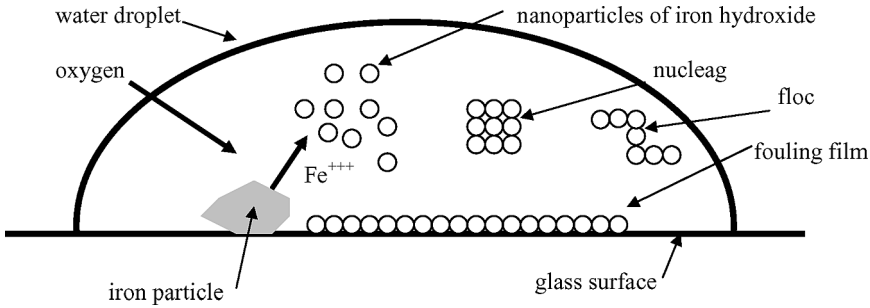

FIGURE 4 Schematic of mechanism for film formation due to corrosion [9].

water and iron can occur, and ferric ions appear in solution. These are rapidly precipitated as the insoluble hydroxide in the form of nanoparticles, which are dispersed under acid conditions. These nanoparticles attract each other slightly and consequently form small metastable nuclei (nucleags), which are continually dissolving and growing in dynamic equilibrium with the suspension. This is a homogeneous nucleation process. Simultaneously, heterogeneous nucleation takes place to form a film of nanoparticles on the glass surface. The nanoparticles and nucleags can subsequently stick together irreversibly to form flocs, which appear as fluffy brown particles visible to the naked eye.

Therefore, fouling film deposition occurs in four stages: 1) by generating a colloidal dispersion of nanoparticles, which exhibit a slight attraction; 2) reversible adhesion of these nanoparticles to nucleate both a fine structured surface coating on the glass and nucleags in suspension; 3) adhesion of the nucleags to form a coarse surface coating film plus large flocs in suspension; and 4) sedimentation of the large flocs to deposit an amorphous fluffy layer.

The adhesion of the nanoparticles may be understood in terms of colloid stability, which depends on the attractive and repulsive forces between the particles. In this analysis, three forces are considered: first, the electrostatic repulsion between charged particles; second, the van der Waals attraction; and third, the thermal motion of the particles, which tends to force the particles apart, as explained in Reference [7]. Each iron hydroxide nanoparticle has a positive charge under acid conditions. This charge causes repulsion of the particles, which overcomes the van der Waals attraction as long as the pH is well below the isoelectric point near pH 7. However, the nanoparticles exhibit a small attractive energy, ε, which is comparable with kT. The nanoparticles also have thermal energy $3kT/2$, which causes

them to collide incessantly and push each other apart. During these collisions, van der Waals attractions can produce adhesive aggregates that are metastable, continually forming and breaking up. The simplest of these aggregates are doublets and triplets, which are not resolved by PCS, but there are also larger metastable aggregates, here called nucleags, which are the nuclei on which further adhesion can occur. These nucleags are similar to the nuclei that allow crystals to grow from a supersaturated solution of ions but are larger for nanoparticles than for ions. They are continually forming because of the slight attraction between particles and continually dispersing because of the thermal energy. The critical size of these nucleags has been calculated from an energy balance theory [12–15]. The diameter, d, was shown to be

$$d = 36D/\{1 + [2.12\,kT\ln(\phi_m/\phi)]/\varepsilon\} \quad (1)$$

where D is the nanoparticle diameter, ϕ is the volume fraction of nanoparticles in suspension, ϕ_m is the packing fraction of particles in the nucleag, ε is the energy of the attractive bond between particles (i.e., the van der Waals attraction minus the electrostatic repulsion), and kT is the Boltzmann energy. Putting in values for the FeOOH nanoparticles, $d = 200$ nm, $D = 20$ nm, $\phi_m = 0.74$, and $\phi = 10^{-4}$, gives the adhesion energy $\varepsilon = 6.8\,kT$. Experiments were conducted with controlled nanoparticle suspensions to verify this theory.

4. FORMING AND CHARACTERISING NANOPARTICLES

FeOOH colloids were prepared by adding $FeCl_3$ solution (filtered at 200 nm) to boiling HCl solution (also filtered at 200 nm) and continuing to boil for 10 min. The pH of the colloid could be controlled by adjusting the amount of HCl in the water. Typically, a dispersion containing 1% by mass of iron chloride was prepared by adding $FeCl_3$ to boiling HCl solution at pH 3.5, and this produced an FeOOH dispersion at pH 2 with a transparent golden colour. This was measured by three laser scattering methods; PCS particle size analysis between 1 and 1000 nm (Malvern HPPS 3.3, Malvern, UK); laser diffraction (LD) from 100 nm upwards (Malvern Mastersizer, Malvern, UK); and direct observation in a laser Tyndall beam.

Results for the 1% FeOOH dispersion at pH 2 are shown in Figure 5. Only one peak is visible around 20 nm in size, and it is clear that this is the dispersed nanoparticle product of reaction. The diameter could be varied by adding the ferric chloride solution to the boiling HCl over different periods of time to nucleate and grow the nanoparticles to different diameters.

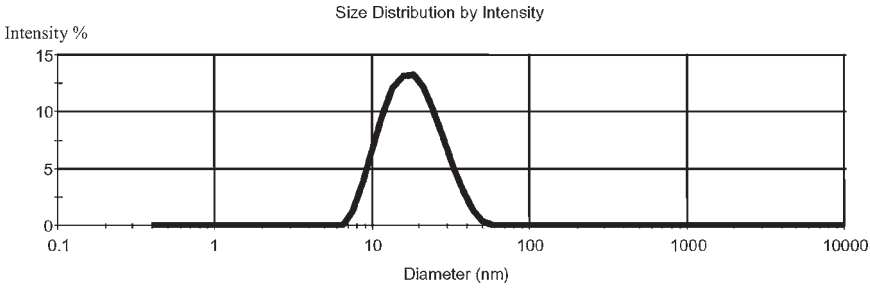

FIGURE 5 Single peak showing the nanoparticles produced by reaction of $FeCl_3$ (1% FeOOH sol at pH 2).

This dispersion was found to deposit fine films on the glass surface of the beaker used in preparation. These films showed the reflection interference colours and exhibited strong adhesion to the glass surface. The conclusion was that nanoparticles of FeOOH could nucleate thin films on glass surfaces under acid conditions. The objective of further experiments was to show how this nucleation was affected by changing pH and surrounding conditions.

The 1% FeOOH dispersion was diluted with filtered deionised water to adjust the conditions towards the realistic corrosion environment of Figure 4, that is pH around 7 and concentration about 2 ppm. At pH 3 and 100 ppm iron concentration, the nanoparticle peak was visible but a new peak could be seen at 160 nm as shown in Figure 6a, growing more prominent on further dilution. This peak was steady with time and appeared to consist of metastable nucleus aggregates of the primary 20 nm particles. We have called these aggregates nucleags to distinguish them from flocs, which are not colloidally stable and which grow with time and then fall to the bottom of the container. On further dilution to 5 ppm, the pH rose to 4.1 and the nucleag peak grew both in particle size and volume (Figure 6b). Lower concentrations of the nanoparticles, less than 5 ppm, were not detected reliably by the instrument.

To follow the changes in aggregation of the nanoparticles, sodium hydroxide solution was added to the dispersion at 100 ppm concentration, giving pH from 2 to 5.4. The results shown in Figure 7 reveal that the nucleags grew steadily in intensity as the pH was increased.

It must be emphasised that the dispersion remained transparent and nonturbid as the aggregates were observed. There was no evidence of flocculation under these conditions, even at pH 5.4. Clearly, the dispersion had not been coagulated by the addition of alkali. The

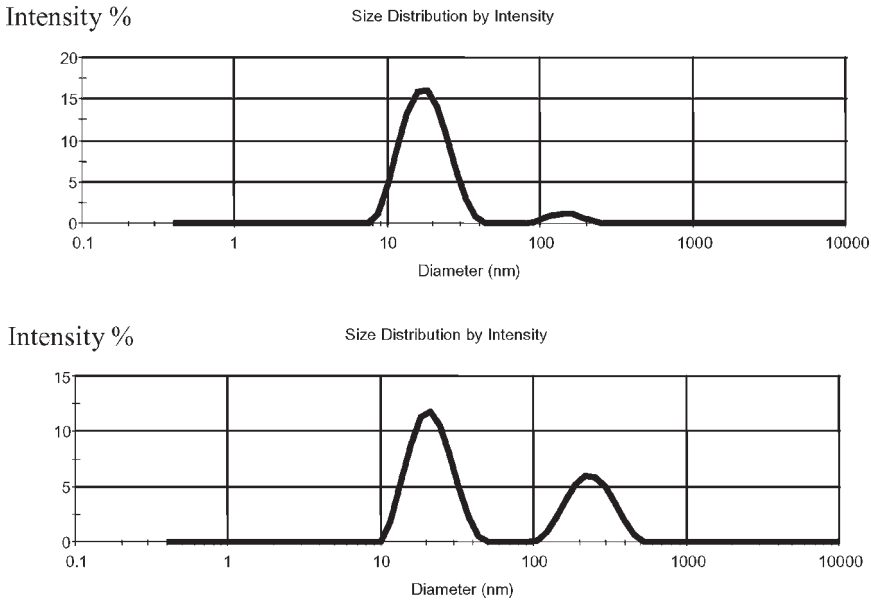

FIGURE 6 Growth of an aggregate peak on diluting the 1% FeOOH sol., first to 100 ppm, pH 3 (top graph), and then to 5 ppm, pH 4.1 (bottom graph).

200 nm aggregates were metastable and growing in concentration as the pH was increased.

However, it was obvious that many dispersed 20-nm particles were present in the sample of Figure 7 bottom, even though the PCS instrument suggested that only 200 nm nucleags were observed. The colour of the suspension did not change significantly at pH 5.4, showing that the dispersion was still dominated by 20-nm nanoparticles. To confirm this the Tyndall beam was used to look at the particles directly. This revealed mainly fine particles with very few nucleags at pH 5.4.

The explanation is that PCS obeys Rayleigh scattering with measured intensity proportional to particle diameter to the power six [11] and proportional to the number of particles, n:

$$I = k\,nD^6 \tag{2}$$

where k is a constant. Because the number of particles is proportional to the mass concentration, C, divided by the cube of diameter, the scattered intensity is given by

$$I = k\,CD^3. \tag{3}$$

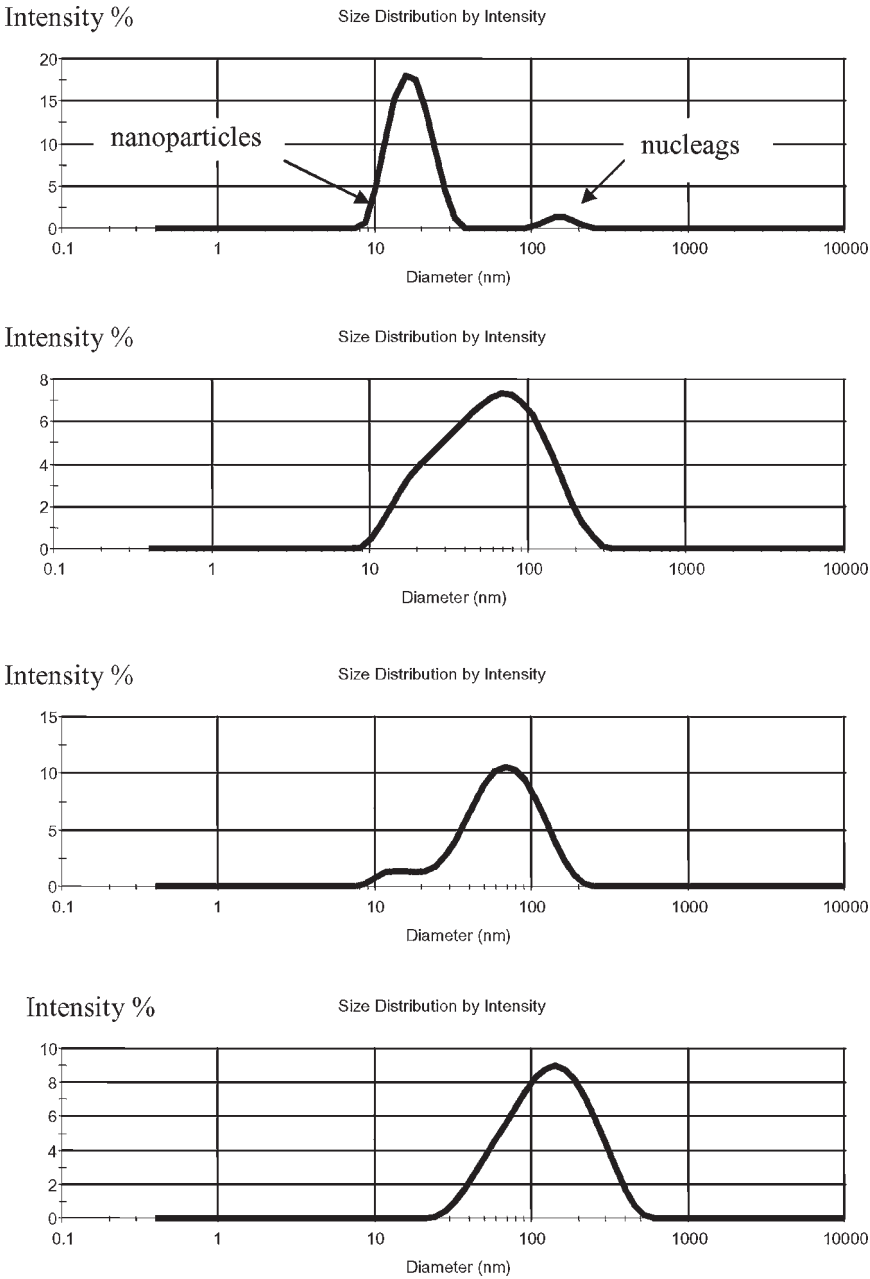

FIGURE 7 Aggregation of nanoparticles at 100-ppm concentration as pH was increased; top, pH 3; next, pH 3.5; next, pH 4; and bottom pH 5.4.

Therefore, the ratio of intensities for the nucleags *versus* the nanoparticles in Figure 7 top is given by the equation

$$I_{\text{nuc}}/I_{\text{nan}} = C_{\text{nuc}}\, D^3_{\text{nuc}}/C_{\text{nan}}D^3_{\text{nan}} \tag{4}$$

Because the left-hand peak in Figure 7 top represents 95% of the intensity and the right-hand peak 5%, $C_{\text{nan}} = 10^{-4}$ by mass, and the ratio of diameters is 10, the concentration of particles by mass causing the right-hand peak calculated from Equation (4) is very small: $C_{\text{nuc}} = 5.10^{-9}$, i.e., 5 ppb. Thus, the PCS method tends to ignore the small particles and is dominated by the larger aggregates. This means it is highly sensitive to the presence of nucleags.

5. FLOCCULATION

As the pH of the dispersion was increased further, above pH 6, flocculation was observed in the suspension and fluffy brown flocs could be seen sedimenting to the bottom of the container. This flocculation process could not be followed using the PCS instrument because Brownian motion is not significant above 1000 nm. Therefore, the Malvern Mastersizer was employed to measure the growth of the flocs. Results are shown in Figure 8 for 100 ppm dispersions at pH 2.6, 3.5, and 5.6.

Figure 8 top shows that the suspension at pH 2.6 contained no flocs and did not alter with time. The primary nanoparticles of 20-nm diameter were too small to be detected by the instrument but the nucleags 800 nm in size were visible. Further growth of the nucleags occurred as the pH was raised to 3.5. Then, as the pH was raised to 5.6, the suspension became turbid and large flocs were observed. The nucleags were not visible because the scattering from the flocs was so large. The Tyndall beam was used to inspect the supernatant liquid at pH 3.5, and it was clear that many nanoparticles and nucleags were still present. At pH 7 the supernatant fluid was very clear and most of the nanoparticles and nucleags had been mopped up by the coagulation.

Thus, it was clear that three types of particles were present in the nanoparticle suspensions, depending on chemical conditions:

1) Nanoparticles dispersed and diffusing, 20 nm in diameter.
2) Nucleags, about 200 nm in diameter, in dynamic equilibrium with nanoparticles. Such nucleags were viewed as metastable nuclei that would grow to flocs on full destabilisation.
3) Flocs that formed irreversibly with time from 1 μm to 100 μm in size. These flocs sedimented to form a brown sludge on the bottom of the container.

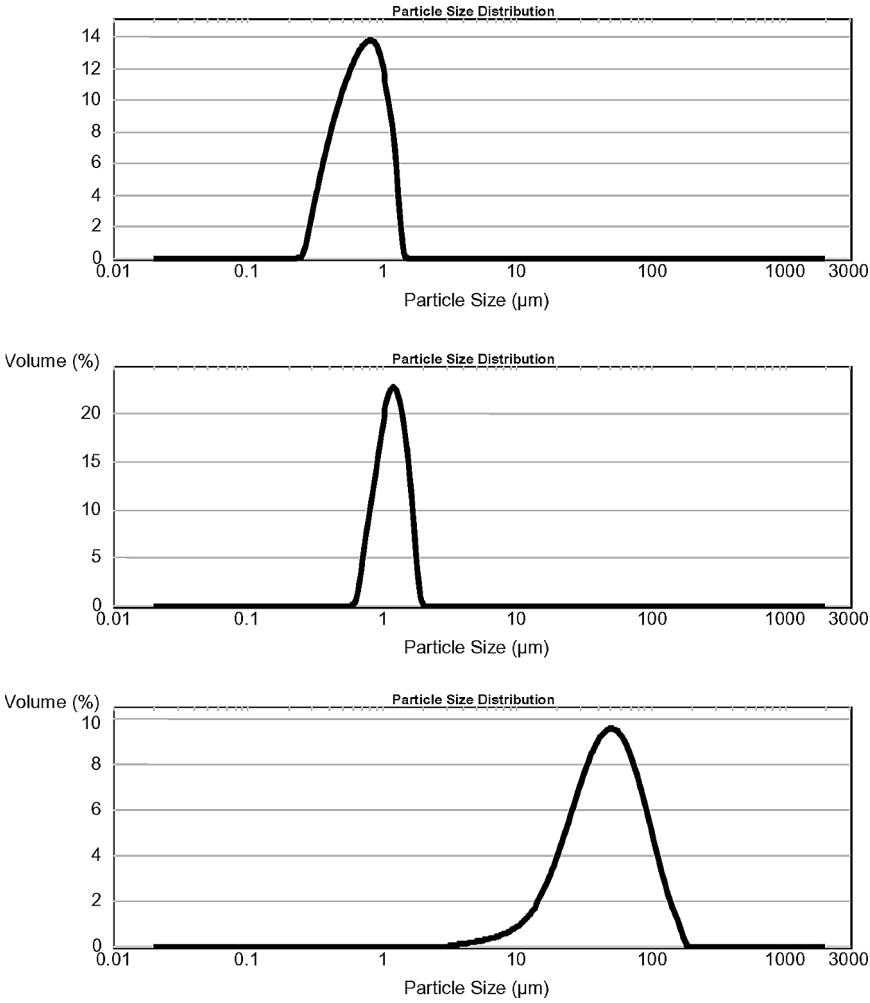

FIGURE 8 Laser diffraction results as pH was increased; top graph, pH 2.6, showing the nucleags; middle graph, pH 3.5, showing flocs; bottom graph, pH 5.6, showing further flocculation.

6. EFFECT OF PHYSICAL CONDITIONS ON FILM FORMATION

It was clear that around pH 3, the colloidally stable FeOOH dispersions were becoming increasingly filled with nucleags, which could form both in suspension and on a smooth surface. The number of nucleags was highly sensitive to pH and to salt concentration. Under these

conditions the suspension was, therefore, extremely sensitive to chemical environment. It was suggested that the nucleags might also be affected by changes in the physical conditions, such as magnetic fields. FeOOH can be a magnetic material, and it is known that magnetic fields cause paramagnetic particles to string together as illustrated in magnetofluids [16].

To demonstrate this idea, a neodymium iron boron sample was cut to fit into the bottom of the PCS instrument cuvette as shown in Figure 9. When this sample was not magnetised, there was no effect

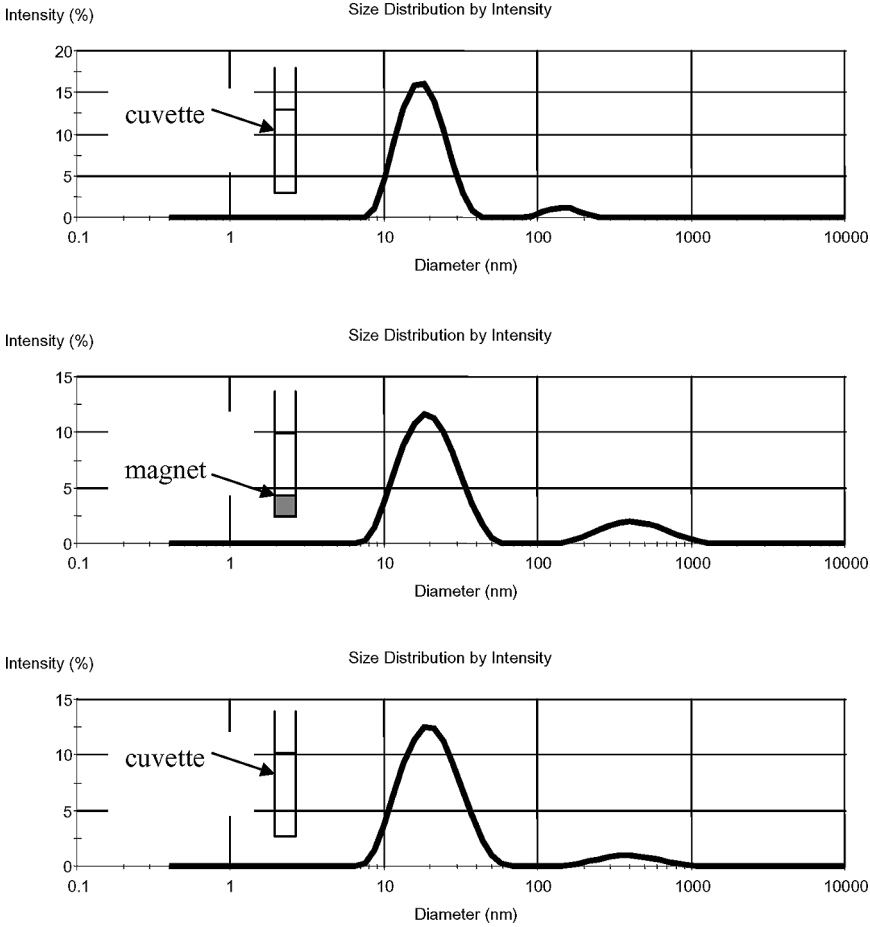

FIGURE 9 Increase in nucleags due to magnet; top, control sample, no field; middle, 1-Tesla field; bottom, after field removal.

observed on the nucleags at pH 3 (Figure 9a). The sample was then magnetised to give a 1-Tesla field and inserted in a cuvette with a 100-ppm FeOOH dispersion at pH 3, which then showed a large increase in both the number and size of nucleags (Figure 9b). It was clear that the magnetic field was adding to the aggregation of the nanoparticles. The magnet was removed and the measurement repeated. The PCS results showed that the nucleags decreased in size and number but not back to their original state, suggesting some irreversibility in the adhesion.

This experiment shows that magnetic fields can have a significant effect on nanoparticle adhesion in suspensions.

7. CONCLUSIONS

This study of nanoparticle adhesion has shown the following:

1) Liquids such as water and kerosene can contain small concentrations of nanoparticles, which can deposit on surfaces to form uniform adhering films.
2) The films can be formed by nucleating films from the fluid suspension under certain colloidal conditions.
3) Nucleation of the film arises both in the liquid and on solid surfaces; 20 nm FeOOH particles form 200 nm metastable aggregate nuclei (called nucleags) in the dispersion, suggesting an interparticle adhesion of about $6.8\,kT$. When the suspension is destabilised, by adding salt or raising pH, then flocs eventually form and irreversible aggregation occurs.
4) The nucleation process is very sensitive to the chemical and physical conditions. In particular, a magnetic field of 1 Tesla increased both the size and the number of nucleags.

ACKNOWLEDGEMENT

Thanks are due to Rex Harris for donating the magnets and advising on their effects.

REFERENCES

[1] Ghatak, A., Mahadevan, L., Chung, J. Y., Chaudhury, M. K., and Shenoy, V., *Proc. R. Soc. Lond.* **A460**, 2725–2735 (2004).
[2] Kohli, R., in *Particles on Surface 7: Detection, Adhesion and Removal*, K. L. Mittal (Ed.) (VSP, Utrecht, 2003), pp. 113–149.
[3] Chow, T. S., *J. Phys: Condensed Matter* **15**, L83–L87 (2003).

[4] Kendall, K., Yong, C. W., and Smith, W., *Proc 27th Annual Meeting of the Adhesion Society*, pp. 58–59 (Adhesion Society, Blacksburg, Virginia, 2004).
[5] Kendall, K., Yong, C. W., and Smith, W., *J. Adhes.* **80**, 21–36 (2004).
[6] Prevo, B. G. and Velev, O. D., *Langmuir* **20**, 2099–2107 (2004).
[7] Kendall, K., *Molecular Adhesion and Its Applications* (Kluwer, New York, 2001), Ch. 10.
[8] Kendall, K., in *Aspects of Adhesion 7*, D. J. Alner and K. W. Allen (Eds.) (Transcripta Books, London, 1973), pp. 173–181.
[9] Kendall, K., *Contem. Phys.* **21**, 277–297 (1980).
[10] Jolivet, J. P., Chaneac, C., and Tronc, E., *Chem. Comm.* March, 481–487 (2004).
[11] Pecora, R., *Dynamic Light Scattering: Applications of Photon Correlation Spectroscopy* (Plenum, New York, 1985).
[12] Kendall, K., Alford, N. McN., Clegg, W. J., and Birchall, J. D., *Nature* **339**, 130–132 (1989).
[13] Kendall, K. and Liang, W., *Brit. Ceram. Trans.* **96**, 92–95 (1997).
[14] Liang, W. and Kendall, K., *Colloids Surf.* **131**, 193–201 (1998).
[15] Kendall, K. and Liang, W., *A New Colloid Phenomenon*, 11 July 1996, www.keele.ac.uk/depts/ch/inorganic/paper.html
[16] Shibayama, A., Otomo, T., Shimada, K., and Fujita, T., 'Measurement of interactive surface force of suspended particles in ER and MR suspensions under electric and magnetic field' in *Electrorheological Fluids and Magnetorheological Suspensions*, Lu, K., Shen, R., and Hon, M. (Eds.) Proc. 9th Int. Conf. Beijing (World Scientific, London, 2004), pp. 163–169.